# Simulation of electric fields generated from microtubule vibrations

Kyle A. Thackston, Dimitri D. Deheyn, and Daniel F. Sievenpiper

Phys. Rev. E **100**, 022410 — Published 15 August 2019

DOI: 10.1103/PhysRevE.100.022410

# Simulation of Electric Fields Generated from Microtubule Vibrations

Kyle A. Thackston,[1,*] Dimitri D. Deheyn,[2] and Daniel F. Sievenpiper[1]

[1] *Electrical Engineering Department, University of California, San Diego.*
[2] *Scripps Institution of Oceanography, University of California, San Diego*

(Dated: July 24, 2019)

Microtubules are tubular proteins that form part of the cytoskeleton in eukaryotic cells. Because of their unique mechanical properties, many studies have theorized microtubules could show high frequency mechanical vibrations. Others have further suggested these vibrations of the electrically polar microtubules could be a source of electric fields inside the cell that could serve some biological function, such as a role in organizing mitosis, or also possibly in cell-to-cell communication. In this work, we use a transient method to simulate the electric fields that would be generated from a single microtubule supposing they could sustain vibrations. We evaluate the biological significance of the electric fields, and the potential energy microtubules might exert on one another. Our simulation method allows us to evaluate vibrational modes that have not previously been studied. The simulations suggest the acoustic branch flexing mode would actually be the most electrically active. Our results suggest a single vibrating microtubule could potentially exert significant forces (those that exceed thermal energy) on biological dipoles or charges at distances larger then the Debye length, on the order of 10 nm from the surface of the microtubule, but interaction is not likely at greater distances.

## I. INTRODUCTION

Microtubules are ubiquitous organelles, appearing in the cytoskeleton of eukaryotic cells. They are tubular protein complexes constructed out of alpha and beta tubulin monomers. Microtubules are highly conserved across different species, and important for functions such as maintaining cell structure, intracellular transport, and cell division [1]. Researchers have spent considerable effort investigating and simulating the high frequency (>kHz) mechanical vibrations naturally exerted by microtubules [2]. One motivation behind this research is the theory that vibrating microtubules are the source of endogenous electric fields, which may serve some biological function [3–6]. The constituent protein tubulin has a net dipole moment, and the arrangement of tubulin in the microtubule is such that the microtubule strand actually has a net dipole moment along its axis. Therefore, the motion of these tubulin proteins would generate alternating electric fields inside the cell.

To date, no experimental evidence has confirmed these high frequency vibrations. Simulation results are mixed in their findings. Many of these computational studies calculate vibrational frequencies on the order of 1 to 100 GHz. These resonant frequencies are dependent on the microtubule length, as are the material properties of the microtubules themselves [2]. One work that used molecular dynamics to identify the normal modes of the microtubule noted that all modes other than flexing (the resonant frequency of which was not dependent on microtubule length) seemed to have lower resonant frequencies for longer microtubules [7]. They also noted that mode number was not length dependent for bending and twisting modes, while axial mode number decreased with increasing length, and flexing mode number increased with increasing length. An approximate model describing microtubule resonant frequency as a function of length is found in [8].

Even if microtubules were able to sustain high frequency mechanical vibrations, however, their ability to generate significant electric fields is not clear. Previous work has modeled electric fields from microtubules undergoing optical branch axial vibrations based on the vibrational analysis of Pokorný [9, 10]. These studies have modeled different arrangements of microtubules using what they have named the Microtubule Resonance Dipole Network Approximation method [8, 11–13].

These previous electric field simulations have only modeled one of the hypothesized vibrational modes from microtubules, namely the optial branch axial vibration. Additionally, it has not been thoroughly investigated whether such theoretical fields could have any biological significance. In this work, we use a transient method to simulate the electric fields from multiple vibrations (optical branch axial, acoustic branch axial, bending, twisting, and flexing). As in other biophysics work, we determine the field strength to be significant when it can interact with a potential energy greater than the background thermal energy [14]. We also evaluate the ability of microtubules to induce vibrations on one another based on their interaction energy.

## II. SIMULATION METHODS

In this work, we will use a numerical transient method to determine the fields generated by microtubule vibrations. Our model is transient in contrast to previous, frequency domain models. We simulate the trajectory of each tubulin monomer over the course of two vibrational

* kthackst@eng.ucsd.edu.

Table I. Dipole moments of tubulin. Note the direction of the dipole moments is presented in cylindrical coordinates, as opposed to the Cartesian coordinate system in the source [16] . Direction of dipole moments defined in Fig. 1.

| Tubulin Dipole Moment (Debye) | $\alpha$ monomer | $\beta$ Monomer |
|---|---|---|
| $P_z$ | 115 | 222 |
| $P_r$ | 554 | 1115 |
| $P_\theta$ | -6 | -192 |

periods in discrete time steps. Our model treats each tubulin monomer as a point dipole and sums the field contributions from each one as they move according to a given equation of motion.

### A. Seeding the Microtubule System

The electromagnetic properties of tubulin and the geometric arrangement of tubulin in the microtubule are fortunately well studied. Although microtubules can be up to 50 µm long, most microtubules are 0.5 µm to 2 µm [1]. The hollow tube of a microtubule has an inner diameter of approximately 15 nm and an outer diameter of approximately 23 nm. In vivo, they consist of 13 protofilaments which wrap around the microtubule with an 8 nm pitch, as depicted in Fig. 1. Typically microtubules form a lattice of tubulin dimers in either the "13A" or "13B" configuration [15]. For the purposes of electric field generation, we have no reason to suspect one lattice type should be more electrically active than the other. In this work, we will consider the "13B" lattice type.

The electrical properties of the alpha and beta tubulin monomers are taken from molecular dynamics simulations and listed in Table I [16]. The dipole moment directions are defined in cylindrical coordinates, as labeled in Fig. 1. The $z$ direction is along the axis of the microtubule, the $r$ direction is directed radially away from the microtubule center, and the $\theta$ direction is tangential to the microtubule surface. Note that while the microtubule does have a net dipole moment along its axis, the radial component of tubulin's dipole moment is the greatest.

### B. Motion of the Microtubule

We simulate five modes of vibrations that have been hypothesized or simulated in previous works. The first four are acoustic branch vibrations: axial, bending, flexing, and twisting [17]. The fifth mode is an axial vibration on the optical branch [9]. The two constituent particles in the microtubule lattice are the alpha and beta tubulin monomers. In acoustic branch vibrations, these monomers move coherently, whereas in optical branch vibrations they move out of phase [18]. For this reason we simulate alpha and beta monomers independently, instead of looking at just the tubulin dimer. Traditionally, optical branch vibrations are considered more electromagnetically active than acoustic branch vibrations, hence the focus on optical branch vibrations in past works.

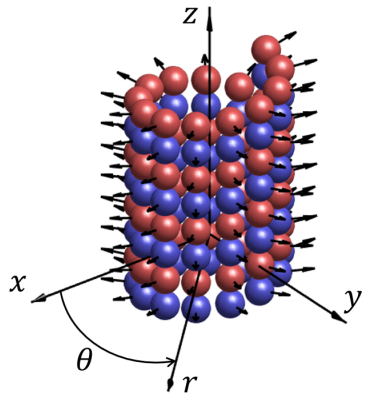


Figure 1. Three dimensional structure of a microtubule. Red spheres indicate alpha tubulin and blue spheres indicate beta tubulin. The black arrows show the dipole moment of each tubulin monomer.

The equations of motion for each mode follow the form of:

$$\xi_i(t) = A\sin(\omega t)\sin\left(\frac{n\pi z_{i0}}{L}\right) + \xi_0 \tag{1}$$

Where $A$ is the amplitude of the vibration, $\omega$ is the angular frequency of the vibration, $n$ is the order of the mode, $L$ is the length of the microtubule, $\xi_i(t)$ is the coordinate dependent on the mode of vibration of node $i$ as a function of time, $\xi_0$ is that same coordinate at $t = 0$, and $z_{i0}$ is the $z$ coordinate at $t = 0$. Every alpha and beta monomer constitutes its own node. The axial, bending, flexing, and twisting modes represent vibrations along the $z$, $x$, $r$, and $\theta$ coordinates respectively (assuming the microtubule is aligned on the $z$ axis, with the base at $z = 0$ and the top at $z = L$, as shown in Fig. 1). In twisting vibrations, the amplitude is scaled to the microtubule radius such that the amplitude of $\theta$ corresponds to the arc length swept. For the optical branch vibration, the beta tubulin monomers are vibrating out of phase with the alpha monomers along the $z$ axis. The motion of Eq. 1 fixes the end points of the microtubule, which would be expected in many biological settings.

Additionally, our simulation applies rotation matrices to the dipole moment of each node at every time step to simulate the deformation of the microtubule. Node $i$ remains in the same orientation to the node directly above it (node $i+13$). These rotation matrices are given by Eq. 2 and Eq. 3, and the angles of rotation are given by Eq. 4.

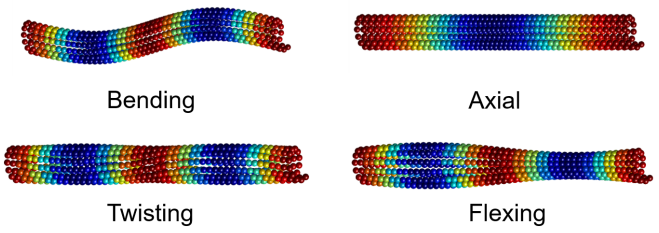


Figure 2. Bending, axial, twisting, and flexing microtubule vibrations (left to right, top to bottom). Amplitudes are exaggerated for the purposes of illustration. All vibrations are second order ($n = 2$).

$$[R_x] = \begin{bmatrix} 1 & 0 & 0 \\ 0 & \cos\theta_x & -\sin\theta_x \\ 0 & \sin\theta_x & \cos\theta_x \end{bmatrix} \tag{2}$$

$$[R_y] = \begin{bmatrix} \cos\theta_y & 0 & \sin\theta_y \\ 0 & 1 & 0 \\ -\sin\theta_y & 0 & \cos\theta_y \end{bmatrix} \tag{3}$$

$$\theta_x = -\tan^{-1}\left(\frac{\Delta y}{\Delta z}\right),\ \theta_y = \tan^{-1}\left(\frac{\Delta x}{\Delta z}\right) \tag{4}$$

The lengths of $\Delta x$, $\Delta y$, and $\Delta z$ are defined as the differences in the $x$, $y$, and $z$ coordinate respectively between node $i$ and node $i + 13$. Thus the dipole moment of any node as a function of time is given by Eq. 5.

$$\vec{p}_i(t) = [R_y][R_x]\vec{p}_{i0} \tag{5}$$

Illustrations of the four acoustic modes, with exaggerated amplitudes, are shown in Fig. 2.

### C. Fields from Microtubule

Because we only consider distances much less than the expected wavelength ($\ll 1\,\text{mm}$), we calculate the total fields using a quasi-static approximation. The electrostatic field from each dipole is summed at every discrete time point in a particular point in space, with the field expression given by Eq. 6 [19].

$$\vec{E} = \frac{3\hat{r}(\hat{r}\cdot\vec{p}) - \vec{p}}{4\pi\epsilon r^3} \tag{6}$$

Where $\vec{E}$ is the electric field strength in V/m, $\vec{p}$ is the vector dipole moment in C m, $\epsilon$ is the permittivity of the medium, and $\vec{r}$ is the distance vector pointing from the center of the dipole to the observation point. In order to enforce the screening effect of the media, which is discussed in greater detail in Appendix A, we simulate the total transient fields at some point in space for a few periods. We remove the DC offset of the field to account for screening and calculate the peak-to-peak electric field strength. This peak-to-peak value is taken as the strength of the $E$ field in the medium. A flowchart depicting how we calculate the electric field in space from the moving microtubules is shown in Fig. 3.

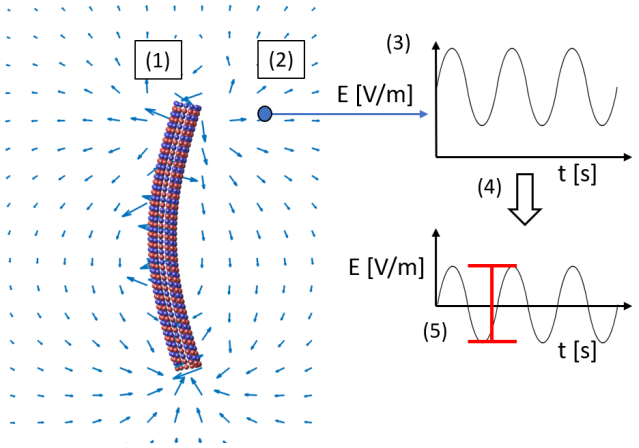


Figure 3. Procedure for numerically calculating the $E$ field strength in conductive media for arbitrary vibrations: (1) Move dipole moments along predetermined motion. (2) Sum fields from all nodes at particular point in space. (3) Get $E$ field vs. time for one point in space. (4) Remove DC component. (5) Extract peak to peak $E$ field.

When we calculate the potential energy in an electric field, we use Eq. 7.

$$U = -\vec{p}\cdot\vec{E} \tag{7}$$

Where $U$ is the potential energy. When we calculate the potential energy between microtubules, we sum the absolute value of the potential energy of every tubulin dimer in the receiving microtubule system in the presence of the fields generated by the transmitting microtubule.

### D. Comparison with Microtubule Resonance Dipole Network Approximation

Our results are slightly different from previous simulations using the Microtubule Resonance Dipole Network Approximation [8, 11–13], which models the the oscillating tubulin as a Hertzian dipole. Here we argue this is not an accurate approximation at larger distances. Just as the time varying fields from an oscillating charge look like a Hertzian dipole, the time varying fields from an oscillating dipole should look like a Hertzian quadrapole. To demonstrate this, let us examine the electric field along the $z$ axis given by a dipole oriented and moving up and down along that same axis.

$$E = \frac{2p}{4\pi\epsilon\big(r + A\sin(\omega t)\big)^3} \tag{8}$$

Where $p$ is the magnitude of the dipole moment, $r$ is the distance between the observation point and the dipole, $A$ is the amplitude of the oscillation, $\omega$ is the angular frequency of vibration, and $t$ is time. If we assume $r \gg A$, we can take the first two terms of the Taylor series expansion of Eq. 8. This isolates the principle component of the time varying fields.

$$E \approx \frac{2p}{4\pi\epsilon r^3} - A\sin(\omega t)\frac{6p}{4\pi\epsilon r^4} \tag{9}$$

The first term in Eq. 9 represents the DC component of the fields, while the second term is time dependent. The time varying fields decay as a power of $r^{-4}$, similar to a Hertzian quadrapole. In conductive media, the DC and low frequency components are screened, as described in Appendix A. Modeling each oscillating tubulin as a Hertzian dipole is therefore overestimating the distance of interaction. We believe our quasi-static transient simulation, which removes the DC fields numerically, is a more accurate simulation.

## III. RESULTS

The key parameters we can sweep in our simulation are the vibration type, mode number, vibration amplitude, the length of the vibrating microtubule, and of course where in space we are measuring field strength. As discussed in Appendix A, we will not consider the impact of vibration frequency as we are only studying near fields from vibrations occurring beyond the Maxwell frequency.

In past works considering the biological effects of electromagnetic fields, significant interaction was deemed to occur at interaction energies greater than thermal energy ($k_BT$), or with forces on the order of 1 pN [14]. The largest dipole moment for a single protein cataloged by [20] is 34,460 Debye (or $1.232 \times 10^{-25}$ C m). From Eq. 7, we can determine the $E$ field necessary to have a potential energy equal to thermal energy ($k_BT$). Assuming a temperature of 300 K, the $E$ field would need a magnitude of 3.36 kV/m. The same database catalogs the largest free charge of any single protein at 446 e. To exert a force of 1 pN would require 1.4 kV/m. This suggests that biologically significant fields must be on the order of 1 kV/m. Here we only consider traditional electromagnetic interaction, ignoring more exotic effects such as stochastic resonance at the receiver which could allow for the reception of weaker signals.

### A. Electric Field from Different Vibration Types

The vibration types studied here are axial, bending, flexing, and twisting modes, as well as optical branch axial vibrations. These are typical normal modes for hollow cylinders and the modes identified in previous computational studies [17]. Any microtubule vibration would consist of some superposition of these modes. Numerical studies suggest all modes have lower resonant frequencies for longer microtubules, except for the flexing mode which has been identified to have a resonant frequency independent of length at about 100 GHz, presumably because the relevant length scale is the microtubule diameter [7]. At these frequencies our model may slightly underestimate the electric fields because the dielectric of cytosol will become frequency dependent.

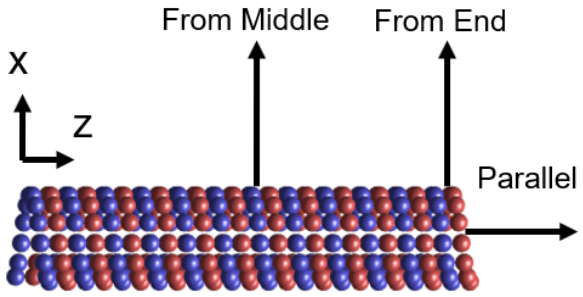


Figure 4. The three different lines along which we plot the $E$ field.

For comparison of vibration type, we simulate the electric field strength as a function of distance perpendicular to the microtubule axis from its middle and end, and distance parallel to the end of the microtubule (illustrated in Fig. 4). All simulations are performed for 1 µm long microtubules with 0.1 nm amplitude vibrations (a typical vibration amplitude according to molecular dynamics works [7]). All vibrations are of the first order ($n = 1$). The dielectric of the media is 80. These results are plotted in Fig. 5. Interestingly, the flexing vibration, which has not been electrically modeled in past works, produces the strongest fields.

### B. Electric Field from varying Mode Order

As the flexing mode produces the strongest fields, we also examine the strength of the $E$ fields for varying mode order in Fig. 6. It has been observed in simulation that mode number was not length dependent for bending and twisting modes, while axial mode number decreased with increasing length, and flexing mode number increased with increasing length [7]. It can be seen that increasing the mode order increases the field strength at close distances, but tends to decrease the field strength at distances that are larger than the scale of the microtubule (1 µm). This trend holds for most other vibrational modes. See Supplemental Figures 1-4 at [URL will be inserted by publisher] for the electric fields of other vibrational modes as a function of mode order.

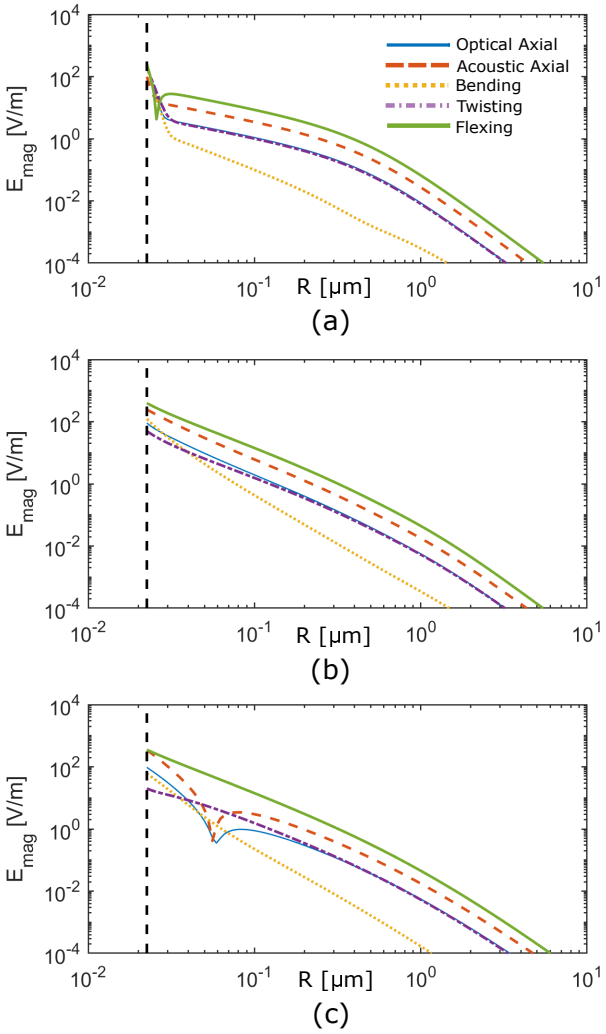


Figure 5. The magnitude of the time varying E fields coming from different vibration types for different orientations labeled in 4. (a) The electric field from the middle of the microtubule. (b) The electric field from the end of the microtubule. (c) The electric field parallel to the microtubule. The black dotted line shows the surface of the microtubule. For all plots, $L = 1\,\mu\text{m}$, $n = 1$, and $A = 0.1\,\text{nm}$.

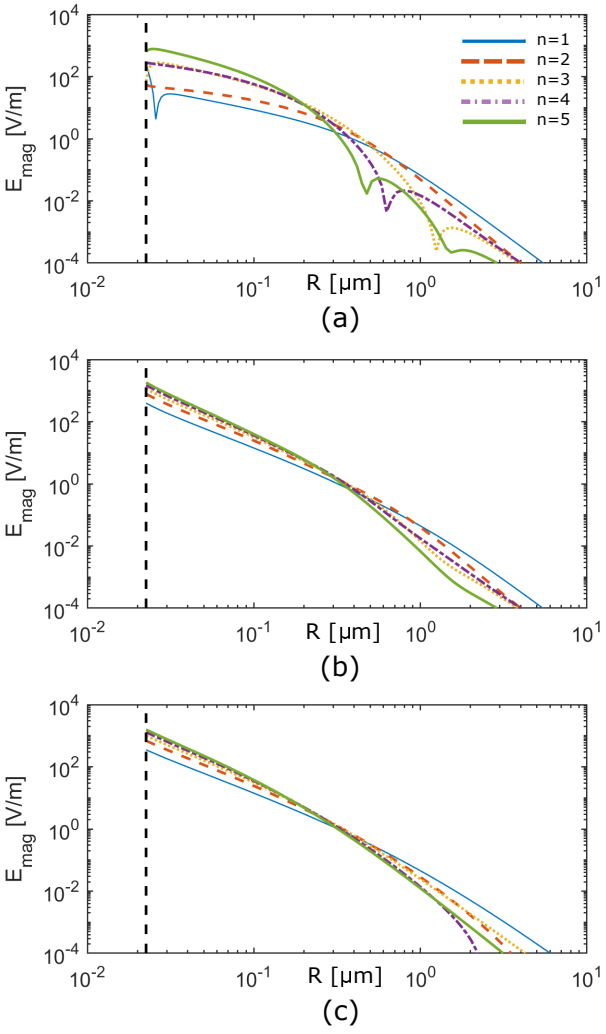


Figure 6. The magnitude of the time varying E fields from a flexing microtubule from different orders of vibration ($n = 1, 2, ...5$) for different orientations labeled in 4. (a) The electric field from the middle of the microtubule. (b) The electric field from the end of the microtubule. (c) The electric field parallel to the microtubule. The black dotted line shows the surface of the microtubule. The black dotted line shows the surface of the microtubule. For all plots, $L = 1\,\mu\text{m}$ and $A = 0.1\,\text{nm}$.

### C. Electric Field as a function of Amplitude

The previous results were simulated with a vibration amplitude of 0.1 nm, on the order predicted by molecular simulation [7]. The same molecular simulations make the intuitive conclusion that amplitude would decrease as vibrational frequency increases, and increase as microtubule length increases. An extrapolated model relating microtubule resonant frequency to length suggests that at lengths larger than 20 µm, the resonant frequency begins to dip below the Maxwell frequency of 250 MHz [17].

To investigate the effects of the amplitude, we plot the electric fields for different amplitudes of the flexing mode from 0.1 nm - 1 nm in Fig. 7. See Supplemental Figures 5-8 at [URL will be inserted by publisher] for the electric fields of other vibrational modes as a function of vibrational amplitude. While longer microtubules should be able to sustain larger amplitudes, vibrations larger than 1 nm seem unlikely without damaging the microtubule. Additionally, we plot the $E$ field at a single point 1 µm

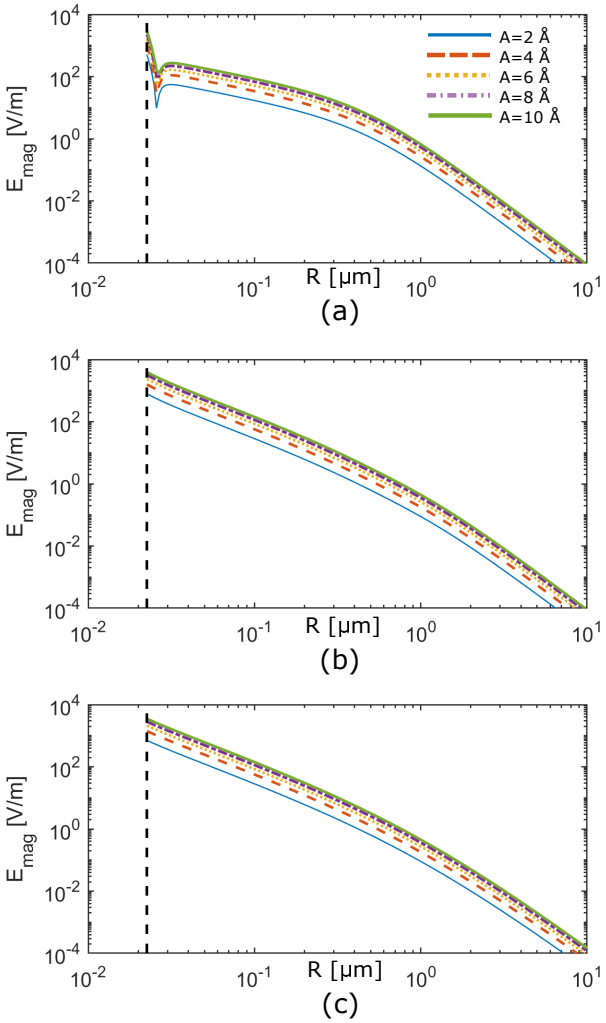


Figure 7. The magnitude of the time varying E fields from a flexing microtubule from varying vibration amplitudes ($A$ = 200 fm, 400 fm, 600 fm, 800 fm, 1000 fm,) for different orientations labeled in 4. (a) The electric field from the middle of the microtubule. (b) The electric field from the end of the microtubule. (c) The electric field parallel to the microtubule. The black dotted line shows the surface of the microtubule. For all plots, $L = 1\,\mu$m and $n = 1$.

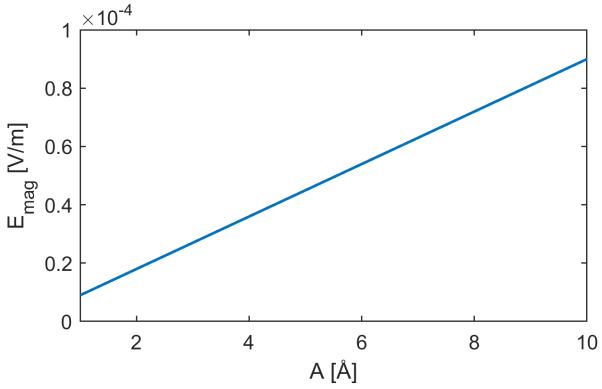


Figure 8. The magnitude of the time varying E fields the middle of a flexing microtubule as a function of vibration amplitude. $L = 1\,\mu$m and $n = 1$.

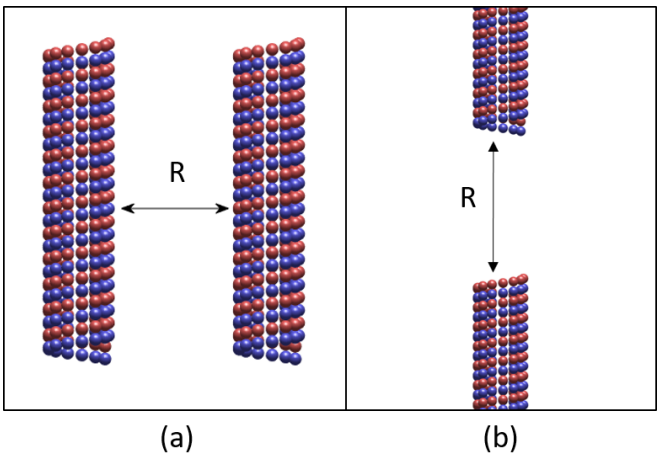


Figure 9. Illustration showing two 100 nm microtubules in parallel (a) and in series (b).

from the middle of flexing microtubule as a function of vibrational amplitude Fig. 8. As expected from Eq. 9, the magnitude of the $E$ field increases linearly with amplitude.

### D. Potential Energy between Two Microtubules

The previous results suggest it would be difficult for the electric fields from a single vibrating microtubule to have significant long range interactions on other biomolecules. To address the question of whether mechanical vibrations in one microtubule could induce vibrations in a neighboring microtubule, we evaluate the potential energy between two microtubules using the process described in section II C. We simulate the potential energy between two shorter microtubules (100 nm long) because the simulation time of our potential energy simulation increases as a function of $L^2$.

We consider two different orientations: two microtubules side by side, and two microtubules along the same axis, as illustrated in Fig. 9. Results are shown for the case of a first order flexing mode with 0.1 nm amplitude vibrations in Fig. 10.

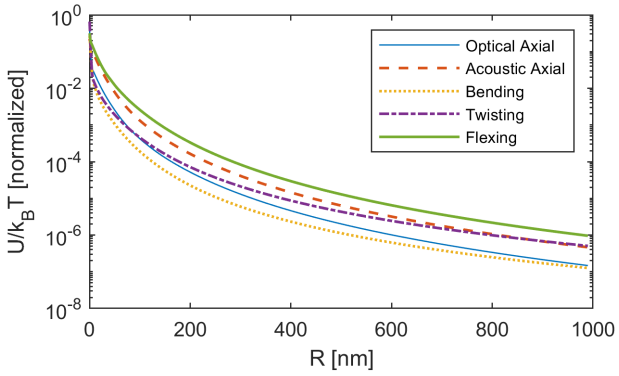


Figure 10. The interaction energy between two microtubules in parallel as a function of distance. $L = 100\,\text{nm}$, $n = 1$, and $A = 0.1\,\text{nm}$.

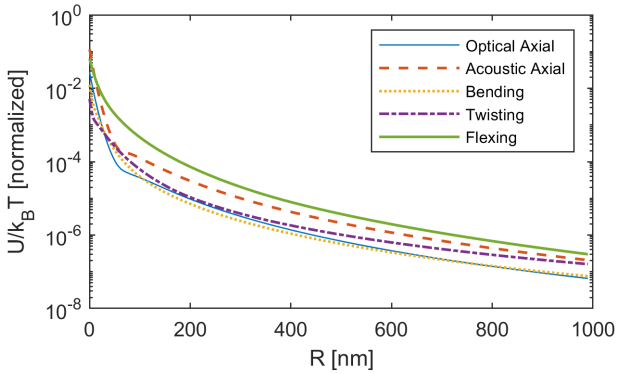


Figure 11. The interaction energy between two microtubules in series as a function of distance. $L = 100\,\text{nm}$, $n = 1$, and $A = 0.1\,\text{nm}$.

## IV. DISCUSSION AND CONCLUSIONS

### A. Different Vibration Types

Earlier we discussed that if an electric field was to interact with biomolecules in any conventional fashion, it would need to be on the order of $1\,\text{kV/m}$ to overcome thermal energy. In Fig. 5 we see that none of the different vibration types achieve fields of that strength for any distance from the microtubule surface. Interestingly, we see the flexing mode is the most electromagnetically active, which has not previously been simulated. This makes sense when noting in table I that the radial component of tubulin's dipole moment is strongest.

Previous works have noted that the axial vibration types are considered the most mechanically likely because they would displace the least fluid and are less likely to be damped [2]. It is also interesting to note that the acoustic axial vibration produces fields stronger than the optical branch axial vibration. Conventional wisdom holds that optical branch vibrations should be more electrically active, and this is true when the constituent particles in the lattice are positive and negative charges. The $\alpha$ and $\beta$ tubulin monomers, however, are dipole moments both with positive $z$ components, instead of opposing charges.

### B. Varying Mode Order and Vibrational Amplitude

Because the flexing mode produced the strongest fields, we evaluated it for different mode orders in Fig. 6. In general we see increasing the mode order results in stronger fields close to the surface of the microtubule, but weaker fields at distances larger than the length of the microtubule. This suggests that the higher order modes would not be useful for long distance interactions.

A physical interpretation of these results is that as the mode order increases, the moment of the effective multipole increases. At distances larger than the length of the microtubule, the vibration should look like a point multipole with some moment proportional to the order of the vibration. As this moment increases, so too will the power at which the fields decay over distance, resulting in weaker fields at distances larger than the length of the microtubule. We also see some dips in the $E$ field around the $1\,\mu\text{m}$ distance only for higher mode orders in the top plot of Fig. 6. We infer this is a location where the field contributions from out of phase oscillations becomes destructive and results in a weaker field.

In Fig. 7 and 8, we swept the vibrational amplitude of the flexing microtubule. As predicted by Eq. 9, the field strength increased linearly with the amplitude. For both the mode order and amplitude sweep, we start to see fields approaching $1\,\text{kV/m}$ at distances on the order of 10-100 nm, significantly longer than the Debye length.

### C. Potential Energy Between Two Microtubules

In Fig. 10 and 11, we simulated the potential energy between two small microtubules for separation distances up to $1\,\mu\text{m}$. As expected, interactions are strongest for the flexing mode. Even when the microtubules are in contact, however, the electric potential energy still cannot surpass the background thermal energy. This suggests it is unlikely that mechanical vibrations in one microtubule could induce vibrations in a neighboring microtubule through electric field interaction.

One issue with this method of simulation is that the mutual energy between two microtubules is dependent on the length of the microtubule. Our simulation method, however, scales in computation with the square of the microtubule length, making simulations of larger microtubules time consuming. Instead of simulating longer microtubules, we derive an analytical model of the potential energy per unit length between two infinite microtubules. The details of the derivation are found in Appendix B. In Fig. 12 we see the models show strong agreement. Two important trends to note from this are that the po-

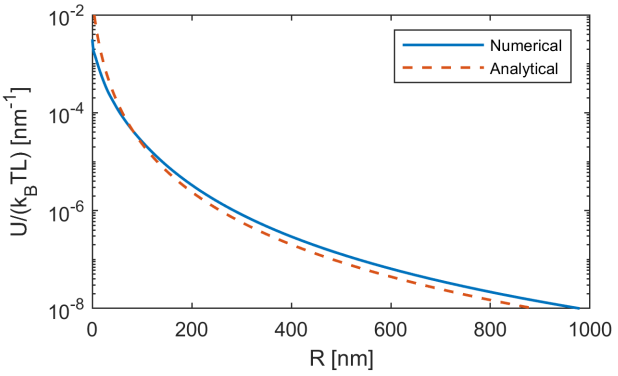


Figure 12. The interaction energy (normalized to thermal energy) per unit length (nm) between two microtubules in parallel as a function of separation distance. The transmitting microtubule is vibrating in the flexing mode. The numerical simulation is from simulating 100 nm long microtubules, while the analytical model assumes the infinite case (see Appendix B for more information on the analytical model).

tential energy decays as a function of $r^{-4}$, and that potential energy between two microtubules scales linearly with length. We see that in order for two microtubules about 50 nm apart to interact above thermal energy in these conditions, the microtubules would have to be approximately 10 µm long.

### D. Summary

We have presented a new method for simulating the electric fields from vibrating microtubules. Our method is capable of simulating any vibrational mode and sweeping a variety of parameters. Based on conventional definitions of interaction, we did not identify any cases where the fields produced by the microtubule could interact with biomolecules at large distances ($> 100$ nm), though there are cases with high vibrational order and amplitude that could achieve fields exceeding 1 kV/m on distances that are at least larger than the Debye length. If these fields were to have any biological significance, they would more likely be for short distance, intracellular regulation, instead of inter-organism communication. Other factors such as multiple coherent microtubules, stochastic resonance at the receiver, or atypical interactions with the media are left outside the scope of this work.

## ACKNOWLEDGMENTS

This work was supported by the Defense Advanced Research Projects Agency under Grant D17AC00022. The content of this article does not necessarily reflect the position or policy of the U.S. Government and no official endorsement should be inferred. Approved for public release; distribution is unlimited.

## Appendix A: Effects of Media on Endogenous Electric Fields

Electrostatic fields are not often considered as long range interactions in cellular systems because of the surrounding ionic medium, such as cytosol. The exponential attenuation of electrostatic fields by the dielectric properties of water and the presence of free charges is typically described as electrostatic screening. Charged or polar molecules will attract an ion cloud around them, canceling out their fields after a few molecular layers. The size of the cloud is characterized by the Debye length of the medium, which is about 1 nm for cytosol [21].

Time varying fields, however, can overcome screening from conductive media at sufficiently high frequencies. Electric fields in dielectrics are attenuated by a factor of $1/\epsilon$, where $\epsilon$ is the dielectric constant of the medium. In conductive media, this dielectric constant becomes complex and is given by $\bar{\epsilon} = \epsilon - i\sigma/\omega$ where $\sigma$ is the conductivity of the medium, $\omega$ is the angular frequency of the field, and $i = \sqrt{-1}$. The ratio of the lossless and lossy dielectric constants gives the attenuation factor of the conductive media.

$$A = \frac{1/\bar{\epsilon}}{1/\epsilon} = \frac{\epsilon\omega}{\epsilon\omega - i\sigma} = \frac{\omega}{\omega - i\omega_0} \tag{A1}$$

$$\omega_0 = \frac{\sigma}{\epsilon} \tag{A2}$$

This attenuation factor given by Eq. A1 implies that for moving charge assemblies, the media acts as a high pass filter with a cutoff around $\omega_0$, also called the Maxwell, or plasma, frequency [22].

For biological solutions such as cytosol, the conductivity is approximately 1.1 S/m and the relative permittivity is about the same as water, which is approximately 80 [23]. This means the Maxwell frequency is approximately 250 MHz [23]. This attenuation is plotted vs. frequency in Fig. 13. For microtubules to be effective sources of electromagnetic fields, we expect them to vibrate near or above the Maxwell frequency. In this work, we assume that vibrations are occurring at a high enough frequency regime where attenuation from conductivity is negligible, other than to remove the DC fields. Given that many computational studies calculate resonant frequencies between 1 to 100 GHz, ignoring the conductivity of the medium other than for the purposes of screening should be a valid assumption [7, 17].

## Appendix B: Analytical Model of Potential Energy Between 2D Microtubules

To give some understanding on the relationship between microtubule length and mutual energy, we derive an analytical model of the mutual energy per unit length

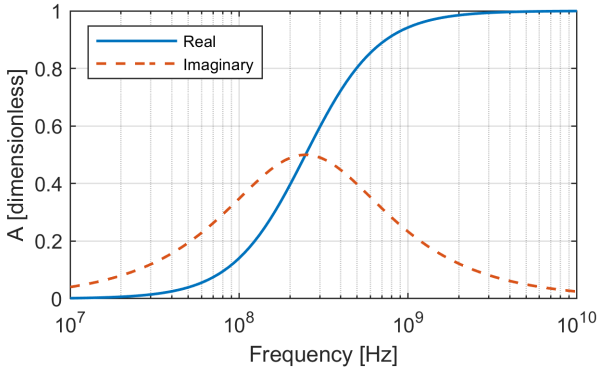


Figure 13. Attenuation factor (given by Eq. A1) of quasi-static electric fields by conductive media when $\epsilon_r = 80$ and $\sigma = 1.1\,\mathrm{S/m}$.

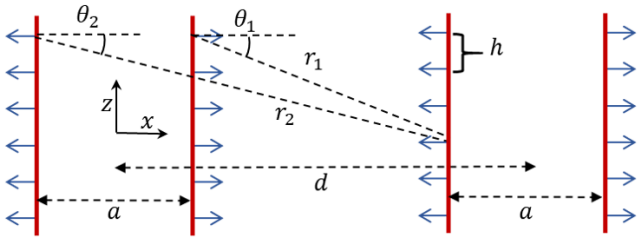


Figure 14. Diagram of the 2D microtubule. Blue arrows represent the radial component of the tubulin dipole. Microtubules have a diameter of $a$ and a separation distance of $d$.

between two infinite, 2D microtubules. A sketch of the problem is shown in Fig. 14.

As discussed in section II D, a dipole moving up and down along its axis creates time varying fields that look like a linear Hertzian quadrapole with a quadrapolar moment given by $Q = Ap$ where $A$ is the amplitude of oscillation and $p$ is the dipole moment. We will model the source as two infinite linearly distributed quadrapoles, where the periodic time dependence is considered implicit. The electric potential from a quadrapole aligned is given by B1.

$$V = \frac{Q}{4\pi\epsilon r^3}(3\cos^2\theta - 1) \tag{B1}$$

Assuming that the microtubule on the left of Fig. 14 is vibrating in the flexing mode (i.e. the dipoles are oscillating along the $x$ axis), we can integrate along the length of microtubule to find the field contribution. Unlike in our numerical simulation, the ends of these microtubules are not fixed, since that would not be meaningful for the infinite case. We can replace $Q$ in B1 with a differential quadrapole moment per unit length given by $\lambda = Ap/h$. Here $h$ is the height of the dipole, in this case 8 nm. The total potential from one side is therefore given by the integral shown in B2.

$$V_i = \int_{-\infty}^{\infty} \frac{\lambda}{4\pi\epsilon r_i^3}(3\cos^2\theta_i - 1)\mathrm{d}z,\ i = 1, 2 \tag{B2}$$

$$\cos\theta_1 = \frac{x-a}{r_1},\ \cos\theta_2 = \frac{x+a}{r_2} \tag{B3}$$

$$r_1^2 = (x-a)^2 + z^2,\ r_2^2 = (x+a)^2 + z^2 \tag{B4}$$

The total potential is simply the sum of the two sides, $V_{MT} = V_1 + V_2$. The electric field is given by $\vec{E} = -\nabla V_{MT}$ and has only an $x$ component.

$$E_x(x) = \frac{\lambda}{4\pi\epsilon}\frac{8x(x^2+a^2)}{(x^2-a^2)^3} \tag{B5}$$

Using 7 as an expression for the potential energy, we can determine the potential energy per unit length for two neighboring microtubules by summing the potential experienced by the left and right side of the microtubule.

$$\bar{U} = \big[E_x(d-a) - E_x(d+a)\big]p/h \tag{B6}$$

After using B5 to solve B6 and recalling our earlier definition of $\lambda$, we can solve for the potential energy per unit length from an infinite vibrating microtubule as a function of separation distance.

$$\bar{U} = \frac{1}{4\pi\epsilon}\frac{Ap}{h}\frac{16p(3ad^2+4a^3)}{h(d^2-4a^2)^3} \tag{B7}$$

We observe that for cases where $d \gg a$, the potential energy is decaying to the power of $d^{-4}$, similar to what was predicted by our numerical case. We expect interaction energy to increase approximately linearly with microtubule length. When plotting B7, we use the numerical values of $p = 1669$ Debye, $h = 8\,\mathrm{nm}$, $A = 0.1\,\mathrm{nm}$, $\epsilon = 80\epsilon_0$, and $a = 23\,\mathrm{nm}$.

[1] A. Akhmanova and M. O. Steinmetz, Control of microtubule organization and dynamics: two ends in the limelight, Nature Reviews Molecular Cell Biology **16**, 711 (2015).

[2] O. Kuera, D. Havelka, and M. Cifra, Vibrations of microtubules: Physics that has not met biology yet, Wave Motion **72**, 13 (2017).

[3] M. Cifra, J. Z. Fields, and A. Farhadi, Electromagnetic

cellular interactions, Progress in Biophysics and Molecular Biology **105**, 223 (2011).

[4] Y. Zhao and Q. Zhan, Electric fields generated by synchronized oscillations of microtubules, centrosomes and chromosomes regulate the dynamics of mitosis and meiosis, Theoretical Biology and Medical Modelling **9**, 26 (2012).

[5] A. D. Ninno and M. Pregnolato, Electromagnetic homeostasis and the role of low-amplitude electromagnetic fields on life organization, Electromagnetic Biology and Medicine **36**, 115 (2017).

[6] J. Pokorn, Physical aspects of biological activity and cancer, AIP Advances **2**, 011207 (2012).

[7] M. A. Deriu, M. Soncini, M. Orsi, M. Patel, J. W. Essex, F. M. Montevecchi, and A. Redaelli, Anisotropic Elastic Network Modeling of Entire Microtubules, Biophysical Journal **99**, 2190 (2010).

[8] D. Havelka, O. Kuera, M. A. Deriu, and M. Cifra, Electro-Acoustic Behavior of the Mitotic Spindle: A Semi-Classical Coarse-Grained Model, PLoS ONE **9**, e86501 (2014).

[9] J. Pokorn, F. Jelnek, V. Trkal, I. Lamprecht, and R. Hlzel, Vibrations in Microtubules, Journal of Biological Physics **23**, 171 (1997).

[10] J. Pokorny, F. Jelinek, and V. Trkal, Electric field around microtubules, Bioelectrochemistry and Bioenergetics **45**, 239 (1998).

[11] M. Cifra, J. Pokorn, D. Havelka, and O. Kuera, Electric field generated by axial longitudinal vibration modes of microtubule, Biosystems **100**, 122 (2010).

[12] D. Havelka, M. Cifra, O. Kuera, J. Pokorn, and J. Vrba, High-frequency electric field and radiation characteristics of cellular microtubule network, Journal of Theoretical Biology **286**, 31 (2011).

[13] O. Kuera and D. Havelka, Mechano-electrical vibrations of microtubulesLink to subcellular morphology, Biosystems **109**, 346 (2012).

[14] R. K. Adair, Biophysical limits on athermal effects of RF and microwave radiation, Bioelectromagnetics **24**, 39 (2003).

[15] L. A. Amos, The microtubule lattice 20 years on, Trends in Cell Biology **5**, 48 (1995).

[16] J. A. Tuszyski, J. A. Brown, E. Crawford, E. J. Carpenter, M. L. A. Nip, J. M. Dixon, and M. V. Satari, Molecular dynamics simulations of tubulin structure and calculations of electrostatic properties of microtubules, Mathematical and Computer Modeling **41**, 1055 (2005).

[17] D. Havelka, M. A. Deriu, M. Cifra, and O. Kuera, Deformation pattern in vibrating microtubule: Structural mechanics study based on an atomistic approach, Scientific Reports **7**, 10.1038/s41598-017-04272-w (2017).

[18] H. Myers, *Introductory Solid State Physics*, 2nd ed. (Taylor and Francis, 1997).

[19] D. J. Griffiths, *Introduction to Electrodynamics*, 1st ed. (Prentice-Hall, 1981).

[20] C. E. Felder, J. Prilusky, I. Silman, and J. L. Sussman, A server and database for dipole moments of proteins, Nucleic Acids Research **35**, W512 (2007).

[21] R. Phillips, J. Kondev, J. Theriot, and H. Garcia, Electrostatics for Salty Solutions, in *Physical Biology of the Cell* (Garland Science, 2013) 2nd ed.

[22] J. R. de Xammar Oro, G. Ruderman, and J. R. Grigera, Electrodynamics of interactions in electrolyte media. Possible consequences in biological functions, Biophysics **53**, 195 (2008).

[23] J. Grigera, F. Vericat, G. Ruderman, and J. R. De Xammar Oro, On the threshold frequency of long-range interactions in physiological solutions, Chemical Physics Letters **156**, 615 (1989).